Structural and magnetic properties of patterned perpendicular media with linearly graded anisotropy

J. Zhang, Z. Sun, J. Sun, S. Kang, S. Yu et al.

Citation: Appl. Phys. Lett. **102**, 152407 (2013); doi: 10.1063/1.4802245
View online: http://dx.doi.org/10.1063/1.4802245
View Table of Contents: http://apl.aip.org/resource/1/APPLAB/v102/i15
Published by the American Institute of Physics.

Structural and magnetic properties of patterned perpendicular media with linearly graded anisotropy

J. Zhang,[1,a)] Z. Sun,[2,a)] J. Sun,[1] S. Kang,[1,b)] S. Yu,[1] G. Han,[1] S. Yan,[1] L. Mei,[1] and D. Li[2,b)]
[1]*School of Physics and State Key Laboratory of Crystal Materials, Shandong University, Jinan 250100, China*
[2]*Department of Electrical and Computer Engineering, Center for Materials for Information Technology, The University of Alabama, Tuscaloosa, Alabama 35487, USA*

(Received 7 March 2013; accepted 4 April 2013; published online 17 April 2013)

$L1_0$-FePt thin films with linearly distributed anisotropy were fabricated by continuously varying substrate temperatures from 650 °C to 290 °C. An average ordering parameter $S = 0.6$ was obtained. The hysteresis loop has a clear bow-tie shape with low remanence and coercivity before patterning. The patterned nanopillar arrays exhibit an enhancement in both remanence and coercivity. Dynamic coercivity measurement shows that the nanopillar arrays with linearly graded anisotropy have a relatively small intrinsic coercivity and a relatively high value of the figure of merit. The switching field exhibits a narrow distribution, which indicates a strong coupling between soft and hard phases in nanopillar arrays with graded anisotropy. © *2013 AIP Publishing LLC* [http://dx.doi.org/10.1063/1.4802245]

The chemically ordered $L1_0$ phase FePt system is an excellent candidate for the future high density magnetic recording media due to its high magnetocrystalline anisotropy energy density (around $\sim 7 \times 10^7$ erg/cc).[1–4] The large crystalline anisotropy of $L1_0$-FePt would allow a thermally stable grain diameter down to 4 nm if fully ordered. However, such high crystalline anisotropy could cause an unfavorable increase in switching field, which may exceed the limitation of writing heads.[5,6] Currently several approaches, such as bit-patterned media, heat- and microwave-assisted recording,[7–12] are under exploration to solve this "trilemma" in magnetic recording. Recently, graded anisotropy materials have received much attention due to their potential applications in bit-patterned media. Theoretical work by Suess and co-workers has demonstrated that the writability of the individual grain can be greatly enhanced by continuously varying the anisotropy between the soft and hard layers.[13–15] However, most experimental works on anisotropy-graded media are focused on the continuous films[16–19] where the magnetization reversal is dominated by domain nucleation and subsequent lateral propagation. It is not suitable to compare results from graded films with the theoretical model, which is based on isolated grains with graded anisotropy and the domain wall propagates from soft to hard ends vertically. Very recently, a little work has been done on the particular Co/Pd system with patterned structures.[20,21] In order to further prove the concept of "graded" anisotropy media, it is highly desirable to experimentally study patterned media with graded anisotropy based on $L1_0$-FePt films.

In this work, we made $L1_0$-FePt films by continuously varying the substrate temperature and then patterned these films into nanopillar arrays by electron-beam lithography (EBL) and ion milling. The original $L1_0$-FePt thin films and patterned nanopillar arrays were systematically studied regards to the structure, magnetic properties, and switching behaviors.

45 nm FePt thin films were deposited on MgO (001) substrates by co-sputtering with Fe and Pt targets. When base pressure reaches to 6×10^{-8} Torr, film deposition starts at an Ar gas pressure of 4 mTorr. The deposition rates of Fe and Pt were 0.828 nm/min and 0.972 nm/min, respectively, which gave the composition of $Fe_{52}Pt_{48}$. The co-sputtered rate of FePt was about 1.92 nm/min. During deposition of FePt, the substrate temperature is gradually changing from 650 °C to 290 °C as the film grew on the MgO substrate. After magnetic film deposition, a 5 nm Ta capping layer was deposited at room temperature, and Ta (5 nm)/FePt (45 nm)/MgO (001) film configuration was obtained. The films were then patterned into magnetic nanopillar arrays with dot size of 87 nm by using JBX-9300FS EBL system and Intelvac ion mill. In EBL patterning, a negative resist hydrogen silsequioxane (HSQ) was spin coated on the magnetic films at a spin speed of 5000 rpm. After exposure and development, magnetic nanopillar arrays were fabricated by ion milling, in which SiOx pillars (as exposed HSQ) with thicknesses of 70–80 nm serve as an etching mask. To obtain strong enough signals from measurements, nanopillar arrays were patterned in an area of 2 mm × 2 mm. The ion mill has an 8 cm Veeco ion source and 10 cm sample stage in diameter, and the beam voltage, accelerating voltage, and beam current were set as 200 V, 60 V, and 65.4 mA, respectively. The crystalline structure of graded films were characterized on X-ray diffractometer using Cu Kα radiation ($\lambda = 1.5405$ Å). The morphology of patterned samples was imaged using a scanning electron microscopy (SEM). Magnetic hysteresis and remanence curves were measured on a Princeton Micromag 2900 alternating gradient magnetometer (AGM) and a superconducting quantum interference device (SQUID).

In order to achieve linearly graded crystalline anisotropy with temperature variation, the magnetic properties of FePt thin films at different substrate temperatures were characterized. A series of 10 nm FePt thin films with uniform anisotropy were grown on MgO (001) substrates at temperatures ranging from 290 °C to 650 °C. Figure 1(a) shows a sequence of X-ray diffraction spectra of deposited thin films at

[a)]J. Zhang and Z. Sun contributed equally to this work.
[b)]Authors to whom corresponding should be addressed. Electronic addresses: dawenl@eng.ua.edu and skang@sdu.edu.cn.

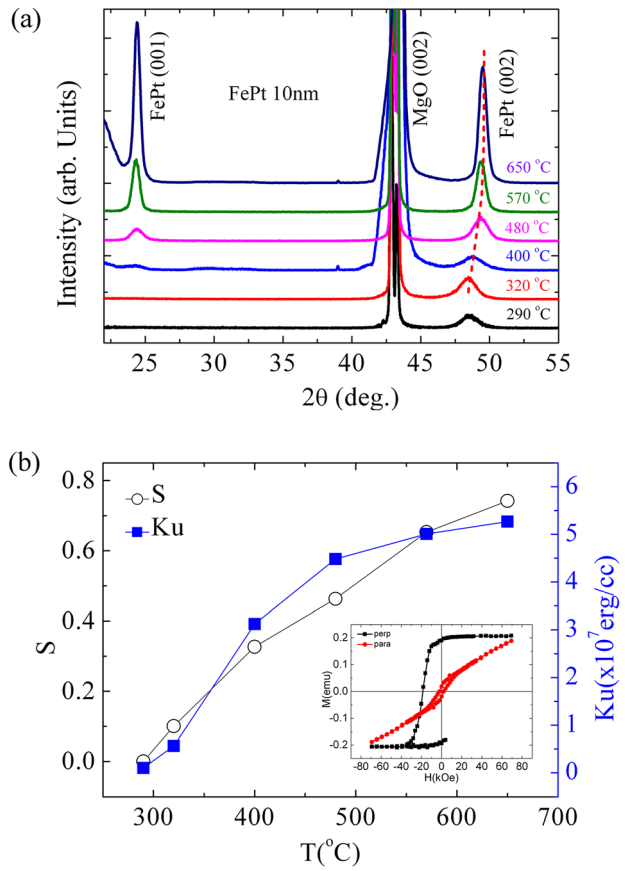

FIG. 1. (a) X-ray diffraction patterns of 10 nm FePt thin films deposited at different substrate temperatures. (b) The dependence of extracted ordering parameter S and the anisotropy constants on substrate temperature. Inset: Hysteresis loops (parallel and perpendicular to the film) of the FePt film grown at 570 °C.

different temperatures. The (001) peak of the face-centered tetragonal FePt (fct) starts to show up at the temperature of 400 °C. As substrate temperature further increases, the intensity of (001) peaks becomes larger and (002) peaks shift to the right simultaneously, which also indicates a phase transition from fcc to fct ($L1_0$ phase). The chemical ordering parameter, S, was extracted based on the ratio of the (001) and (002) peak integrated intensities in XRD spectra, as given in the following equation:

$$s^2 = \frac{(I_{(001)}/I_{(002)})_{obs}}{(I_{(001)}/I_{(002)})_{cal}}, \quad (1)$$

where $(I_{(001)}/I_{(002)})_{obs}$ is the ratio from experimental XRD measurements, while $(I_{(001)}/I_{(002)})_{cal}$ is the theoretically calculated ratio for perfect chemically ordered FePt alloy.[22] Figure 1(b) shows that the ordering parameter is dependent on the substrate temperature, and S monotonously increases with the substrate temperature. Since the highest substrate temperature is 650 °C, the maximum ordering parameter achieved is about 0.8, indicating all samples are partially chemically ordered. Here, we should mention that the contribution from the grains with C-axis lying in the film plane is not considered for calculating *S parameter*. This may result in a slight underestimate of S for the samples grown at low temperature, where fct-FePt (002), fct-FePt (200), and/or fcc-FePt (200) peaks have an overlap. However, for the samples grown at high temperature, the fct-FePt (200) peak is hard to be observed; therefore, S parameter was estimated without considering this peak. Figure 1(b) also shows that the anisotropy constant calculated from the equation $K_u = H_K \cdot M_S/2$ is a function of the substrate temperature, where the switching field H_K is derived from the extrapolation of unsaturated hard axis loops as shown in the inset of Figure 1(b). A high substrate temperature results in an increased crystalline anisotropy due to enhanced chemical ordering of FePt alloy. Based on the correlation between anisotropy and deposition temperature shown in Figure 1(b), the 45 nm FePt thin films with a linearly distributed anisotropy from 5.27×10^7 erg/cc to 1.1×10^6 erg/cc were deposited by continuously varying substrate temperature from 650 °C to 290 °C with a thickness interval of 2 nm. Meanwhile, based on the co-sputtered rate of FePt, the temperature was hold for about 63 s during each interval. The corresponding relationship between the substrate temperature and the anisotropy constant was set up by interpolating the K_u versus temperature curve in Figure 1(b). Deposition temperature reduction at every 2 nm can ensure linearly distributed anisotropy because the 2 nm thickness interval is smaller than the domain wall width of $L1_0$-FePt films. As shown in Figure 2, the anisotropy of upper layer is lower than the under layer because of reduced temperatures in film deposition from the bottom towards the top end. Comparing the XRD spectrum of FePt film with linearly graded anisotropy with the film with uniform anisotropy (substrate temperature fixed at 650 °C) in Figure 2, it is obvious that the (001) peak to (002) peak intensity ratio of FePt film with graded anisotropy is less than that of FePt film with uniform anisotropy. The average ordering parameter, S, calculated from Eq. (1) is about 0.6 for FePt film with graded anisotropy, smaller than that of FePt film with uniform anisotropy.

As shown in Figure 3(a), the patterned nanopillar arrays are well-ordered, and the diameter of nanopillar is about 87 nm and the pitch size (central distance between nanopillars) around 100 nm. Figure 3(b) shows the easy-axis (out-of-plane) hysteresis loops of as-made 45 nm FePt films and patterned nanopillar arrays with linearly graded anisotropy. For comparison, the easy-axis hysteresis loops of as-made films with uniform anisotropy and patterned nanopillar arrays

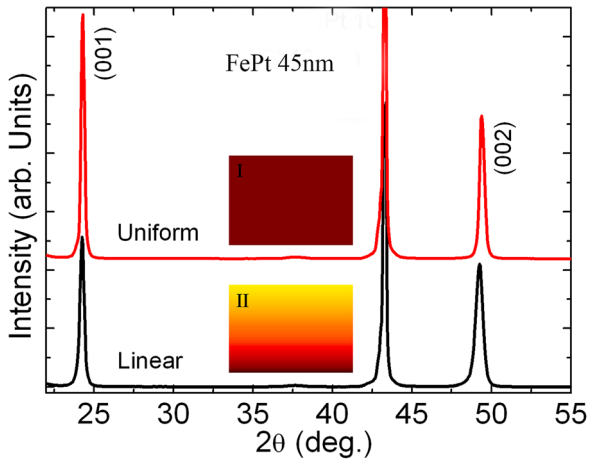

FIG. 2. Comparison of XRD patterns between FePt films with linearly graded anisotropy and uniform anisotropy. Insets: Schematics of FePt films with (I) uniform anisotropy and (II) linearly graded anisotropy, respectively.

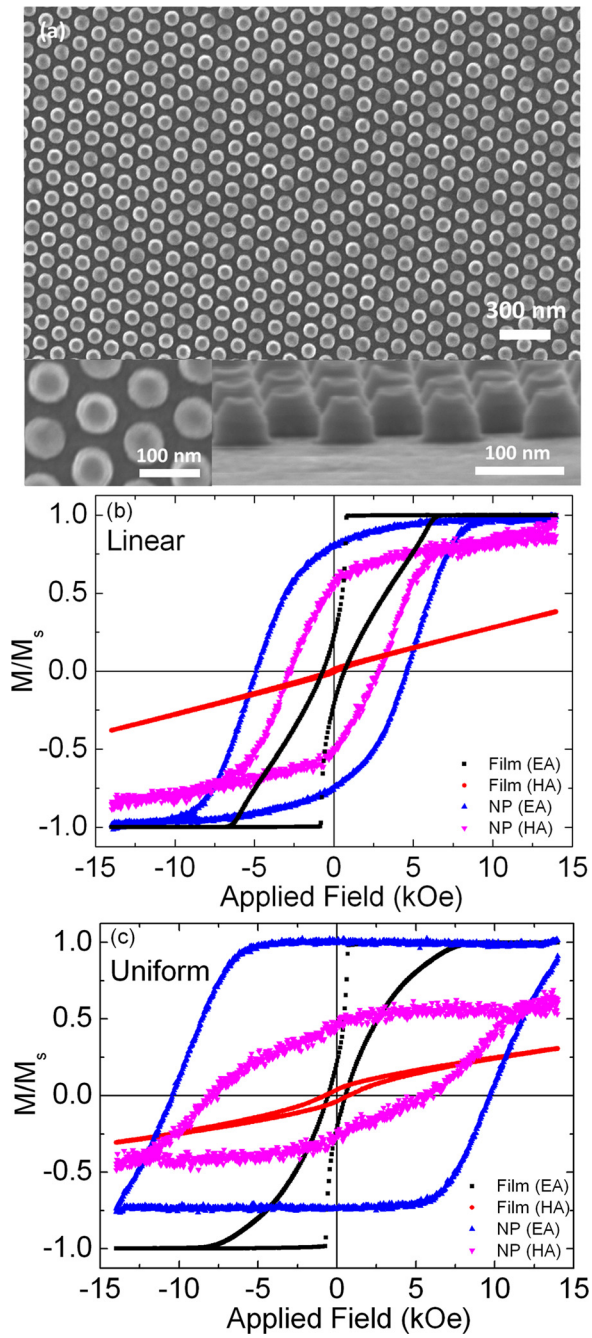

FIG. 3. (a) SEM image of patterned nanopillar arrays with linearly graded anisotropy. Easy-axis (EA) and hard-axis (HA) hysteresis loops of as-made FePt films and patterned nanopillar (NP) arrays, (b) with linearly graded anisotropy, and (c) for uniform anisotropy case.

are presented in Figure 3(c). The easy-axis loops for both films have clear bow-tie shapes with low remanence and coercivity, which indicates that the magnetization reversal is dominated by domain wall propagation. The nanopillar arrays exhibit an enhancement in both remanence and coercivity. The shapes of easy-axis hysteresis loops from the patterned nanopillar arrays suggest a nucleation at the beginning, followed by rapid domain wall motion. The coercivity of the nanopillar arrays with graded anisotropy is smaller than that of the uniform ones. The hard-axis loops for both patterned samples exhibit minor loops and are hard to be saturated.

The magnetic properties of patterned nanopillar arrays with both uniform anisotropy and linearly graded anisotropy are further characterized by the temperature-dependent coercivity measurement as shown in Figure 4. The smooth curves through the experimental data result from the least-square fit using Sharrock's formula,[23]

$$H_{cr} = H_0\left\{1 - \left[\frac{k_B T}{K_u V}\ln(f_0 t)\right]^n\right\}, \tag{2}$$

where H_0 is the intrinsic, short-time coercivity at temperature of zero Kelvin, K_u is the anisotropy energy density, V is the magnetic switching volume, k_B is Boltzmann's constant, T is the absolute temperature, f_0 is the attempt frequency ($\sim 10^9$ Hz for single phase media and $\sim 10^{12}$ for exchange coupled or graded media[24]), and t is the wait time at reverse field. Here, the single phase media model and exchange coupled media model are used for the samples with uniform anisotropy and linearly graded anisotropy, respectively. Therefore, the exponent n should be 1/2 and 2/3 for the nanopillar arrays with uniform anisotropy and linearly graded anisotropy, respectively.[24] Intrinsic coercivity H_0 and the thermal stability factor K_uV/k_BT were obtained through fitting the temperature dependence of the remanent coercivity using Eq. (2). As shown in Figure 4, the patterned FePt nanopillar arrays with uniform anisotropy exhibit a larger H_0 compared to nanopillar arrays with linearly graded anisotropy, because the FePt nanopillar arrays with uniform anisotropy have a higher chemical ordering than that with linearly graded anisotropy. In addition, the thermal stability was characterized at room temperature. The calculated thermal stability factors K_uV/k_BT of the FePt nanopillar arrays with uniform anisotropy are a little bit larger than that of the FePt nanopillar arrays with linearly graded anisotropy. The K_uV/k_BT, for both samples are beyond 100, indicating that the magnetization could be stable for more than a decade. It should be noted that the temperature dependent measurement gives a slightly lower value of K_uV/k_BT due to the temperature dependence of K_u.[25] Furthermore, the calculated relative figure of merit ($\xi = 2\Delta E/(M_S H_{SW} V)$) for FePt nanopillar arrays with linearly graded anisotropy is 61% larger than that of the FePt nanopillar arrays with uniform anisotropy from the temperature-dependent remanent coercivity

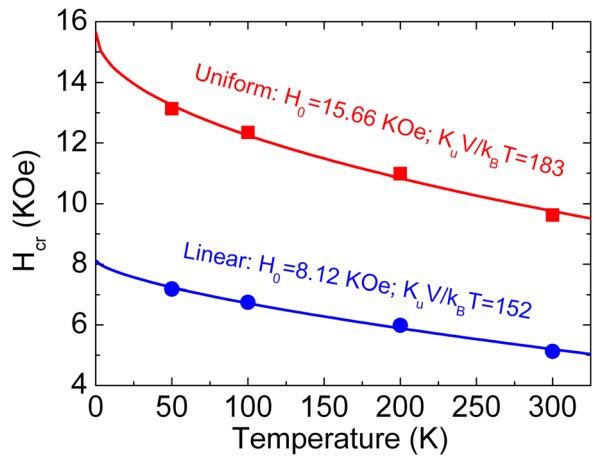

FIG. 4. The temperature dependence of the remanent coercivity for patterned FePt nanopillar arrays with both uniform anisotropy and linearly graded anisotropy. Lines are theoretical fitting based on Eq. (2). The thermal stability factors were obtained at room temperature.

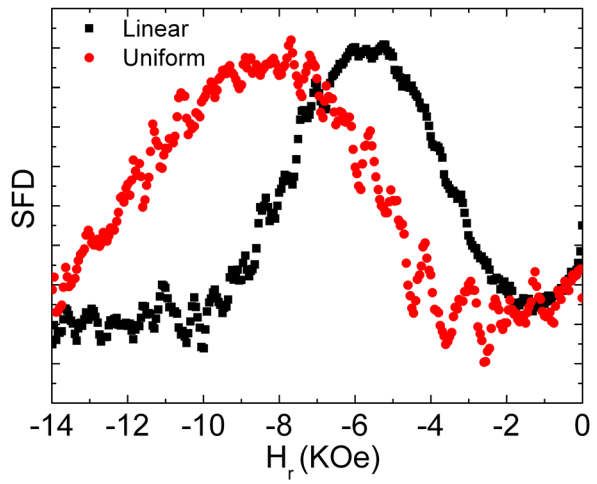

FIG. 5. SFD obtained from DCD curves for patterned FePt nanopillar arrays with both uniform anisotropy and linearly graded anisotropy.

measurement, demonstrating the benefit of graded anisotropy materials for ultra-high-density magnetic recording media.

Figure 5 illustrates the switching field distribution (SFD) obtained from direct current demagnetization (DCD) remanence curves for patterned FePt nanopillar arrays with uniform anisotropy and linearly graded anisotropy. The broad peak for FePt nanopillar arrays with uniform anisotropy corresponds to the nucleation and propagation of the domain walls ranging from the small to the large external fields. Nevertheless, the SFD for FePt nanopillar arrays with linearly graded anisotropy exhibits a relatively narrow peak, which indicates that the soft and hard phases in the sample are strongly coupled. In general, the distribution of size, anisotropy, and easy axis will broaden the SFD. For our patterned nanopillar arrays, the size distribution is very narrow as shown in Fig. 3(a). If the soft phase and hard phase of nanopillar arrays with linearly graded anisotropy are not well coupled, it will result in a broad SFD due to the linear distribution of anisotropy. For the nanopillar arrays with uniform anisotropy, the broad SFD may be partially due to the easy axis distribution. However, as indicated from Figure 5, the switching field from nanopillar arrays with linearly graded anisotropy is less than that from uniform ones, which demonstrates easier nucleation and propagation of domain walls in graded FePt nanopillar arrays, benefitting overall switching behavior.

In summary, we studied the structural and magnetic properties of 45 nm $L1_0$-FePt thin films and patterned nanopillar arrays with linearly graded anisotropy. It has been found that both coercivity and remanence are increased after patterning. Compared with uniformly graded media, nanopillar arrays with linearly graded crystalline anisotropy demonstrate a reduced switching field while a good thermal stability is maintained.

This work has been supported by the National Natural Science Foundation of China (Grant Nos. 50971080, 11174183, and 50901043), the program for New Century Excellent Talents (NCET-10-0541), 111 Project B13029, and the Scientific Research Foundation for Returned Overseas Chinese Scholars from National Education of Ministry and Natural Science Foundation of Shandong (Grant No. JQ201201). D. Li and Z. Sun gratefully acknowledge the financial support from NSF grant (ECCS - 0901858) and graduate student scholarship from MINT Center.

[1]D. Weller, A. Moser, L. Folks, M. E. Best, W. Lee, M. F. Toney, M. Schwickert, J. U. Thiele, and M. F. Doerner, IEEE Trans. Magn. **36**, 10 (2000).
[2]S. Sun, C. B. Murray, D. Weller, L. Folks, and A. Moser, Science **287**, 1989 (2000).
[3]Z. R. Dai, S. H. Sun, and Z. L. Wang, Nano Lett. **1**, 443 (2001).
[4]S. Kang, J. W. Harrell, and D. E. Nikles, Nano Lett. **2**, 1033 (2002).
[5]H. Jiang, K. Sin, and Y. J. Chen, IEEE Trans. Magn. **41**, 2896 (2005).
[6]Y. Kanai, S. J. Greaves, K. Yamakawa, H. Aoi, H. Muraoka, and Y. Nakamura, IEEE Trans. Magn. **41**, 687 (2005).
[7]R. H. Victora and X. Shen, IEEE Trans. Magn. **41**, 537 (2005).
[8]T. W. McDaniel, J. Phys. Condens. Matter. **17**, R315 (2005).
[9]J. G. Zhu, X. C. Zhu, and Y. H. Tang, IEEE Trans. Magn. **44**, 125 (2008).
[10]M. H. Kryder and R. W. Gustafson, J. Magn. Magn. Mater. **287**, 449 (2005).
[11]H. J. Richter, IEEE Trans. Magn. **35**, 2790 (1999).
[12]Z. Sun, D. Li, A. Natarajarathinam, H. Su, and S. Gupta, J. Vac. Sci. Technol. B **30**, 031803 (2012).
[13]D. Suess, T. Schrefl, S. Faehler, M. Kirschner, G. Hrkac, F. Dorfbauer, and J. Fidler, Appl. Phys. Lett. **87**, 012504 (2005).
[14]D. Suess, Appl. Phys. Lett. **89**, 113105 (2006).
[15]D. Suess, J. Fidler, G. Zimanyi, T. Schrefl, and P. Visscher, Appl. Phys. Lett. **92**, 173111 (2008).
[16]Y. Choi, J. S. Jiang, Y. Ding, R. A. Rosenberg, J. E. Pearson, S. D. Bader, A. Zambano, M. Murakami, I. Takeuchi, Z. L. Wang, and J. P. Liu, Phys. Rev. B **75**, 104432 (2007).
[17]B. J. Kirby, S. M. Watson, J. E. Davies, G. T. Zimanyi, K. Liu, R. D. Shull, and J. A. Borchers, J. Appl. Phys. **105**, 07C929 (2009).
[18]J. Lee, V. Alexandrakis, M. Fuger, B. Dymerska, D. Suess, D. Niarchos, and J. Fidler, Appl. Phys. Lett. **98**, 222501 (2011).
[19]C. L. Zha, R. K. Dumas, Y. Y. Fang, V. Bonanni, J. Nogues, and J. Akerman, Appl. Phys. Lett. **97**, 182504 (2010).
[20]J. E. Davies, P. Morrow, C. L. Dennis, J. W. Lau, B. McMorran, A. Cochran, J. Unguris, R. K. Dumas, P. Greene, and K. Liu, J. Appl. Phys. **109**, 07B909 (2011).
[21]B. J. Kirby, J. E. Davies, K. Liu, S. M. Watson, G. T. Zimanyi, R. D. Shull, P. A. Kienzle, and J. A. Borchers, Phys. Rev. B **81**, 100405 (2010); B. Fu, J. W. Harrell, and G. B. Thompson, IEEE Magn. Lett. **3**, 4500404 (2012).
[22]A. Martins, M. C. A. Fantini, and A. D. Santos, J. Magn. Magn. Mater. **265**, 13 (2003).
[23]M. P. Sharrock, J. Appl. Phys. **76**, 6413 (1994).
[24]M. Kapoor and R. H. Victora, IEEE Trans. Magn. **43**, 2289 (2007); J. Dean, M. A. Bashir, A. Goncharov, G. Hrkac, S. Bance, T. Schrefl, A. Cazacu, M. Gubbins, R. W. Lamberton, and D. Suess, Appl. Phys. Lett. **92**, 142505 (2008).
[25]S. Kang, Z. Jia, D. E. Nikles, and J. W. Harrell, IEEE Trans. Magn. **39**, 2753 (2003).